Energy Equip. Sys./ Vol. 11/No. 1/March 2023/ 95-122

ENERGY EQUIPSYS

Energy Equipment and Systems
http://energyequipsys.ut.ac.ir
www.energyequipsys.com

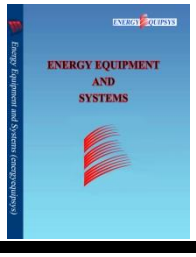

Proposal of a novel ammonia brayton cycle integrated with a methane/hydrogen brayton cycle; Thermodynamic and environmental impacts assessments

Authors
Alireza Pirmohamadi[a*]
Behrooz M. Ziapour [a]

Department of Mechanical Engineering, University of Mohaghegh Ardabili, P.O. Box 179, Ardabil, Iran

Article history:

Received : 4 December 2022
Accepted : 27 January 2023

ABSTRACT

In recent decades, the environmental concerns about utilization of fossil fuels in energy systems have convinced the researchers to chase and employ the carbon-free fuels. Ammonia, regardless of its higher combustion temperature and the significant NOx emission is considered as a promising type of carbon-free fuels, which improving its chemical properties would introduce it as an excellent heat source of power plants. In present study, the proposal of series of ammonia and methane/hydrogen Brayton cycles connected through the exhaust gas recirculation (EGR) unit was investigated. The EGR unit allowed the overall combined cycle to run with the least value of carbon dioxide and NOx. Hence, the chemical and thermodynamic analyses were carried out to yield the optimum molar fractions of fuel mixture, which resulted in lower combustion temperature, higher thermal efficiency as well as specific work. Focusing on the equivalence ratio (φ) as the key parameter in this study, the results showed that under operating conditions, the overall thermal efficiency improved from 63% to 74%, while the remarkable efficiency improvements in all the three subordinate cycles was observed. In addition, the specific work of overall system showed 80% improvement by 1000 kJ/kg. Furthermore, injection the hydrogen to methane combustion could illuminate the carbon dioxide near to zero. Besides, finding the optimum molar fractions of ammonia-air mixture under the rich region diminished the NOx emission from about 1000 ppm down to 10 ppm in $1 < \varphi < 1.2$ *. This index in lean region was decreased from 2500 ppm to 1200 ppm.*

Keywords: Integration, EGR, Equivalence Ratio, NOx Emission.

1. Introduction

In recent years, the flexibility of fuel is one of the interesting fields of research in energy systems. The zero or low carbon dioxide resources are currently being extensively scrutinized, and the purpose of such researches is to explore the clean sources with high output power and low pollution with the less negative impacts on climate change. At the moment, ammonia has been proposed as a promising candidate with the mentioned energetic as well as environmental features, and among the common fuels, it is believed more economical than pure hydrogen [1]. Another reason for partiality of ammonia to hydrogen is its reliability and safety in liquefaction and storage [2], [3]. Ammonia can be pressurized at the

* Corresponding author: Alireza Pirmohamadi
Department of Mechanical Engineering, University of Mohaghegh Ardabili, P.O. Box 179, Ardabil, Iran
Email: pirmohamadi.ar@gmail.com

reference temperature up to 1 MPa [4], also there has been existing infrastructure to develop this novel energy carrier, such as storage and transportation, which makes the ammonia practice conveniently [5], [6], [7]. Furthermore, some literature discuss on negative points on ammonia among them, serious health problems once inhaling and its rule in global warming [8]. As a fuel, ammonia has a great potential to drive the gas turbine system, then this matter captivated many attentions, and many studies have been conducted on the features of ammonia from various point of views which among them the combustion is very crucial subject [9], [10], [11].

Subject of ammonia combustion as a key factor for utilizing this fuel in gas turbine systems. As higher combustion temperature and huge value of NOx among the combustion products is released, most of the researches on ammonia for power generation is contributed on behavior of flame inside the burner. Progress of flame inside the combustion chamber and its control are the crucial design parameters which convinced the researchers to focus on. In addition, numerous studies on carbon fuels such as hydrogen, ammonia and their environmental impacts have been conducted over the past years. Hence, some of the notable studies on mentioned subjects are presented in brief. Karabeyoglu et al. [12] inspected the concerns on the application of ammonia in energy systems. In addition, they considered the negative parameters such as health safety and the lower energy density of ammonia. They discussed the equipment through which the combustion of ammonia are feasible along with the least NOx emission. Grcar et al. [13] focused on the chemical analysis of ammonia inside the combustors. They compared the results of high and low temperature reactions and resulted that NOx release is diminished in high temperatures in non-premixed region of fuel mixture.

Ahlgren [14]studied the density of different fuels and concluded that the nuclear based ammonia as a carbon free fuel holds the less negative environmental impacts. Similarly, Bicer et al. [15] investigated the comparative life cycle assessment study. Also, focusing on density of various alternative fuels, they showed the preference of ammonia and methanol respect to the other proposing fuels.

Bozo et al. [16] modeled a multigeneration energy system which was derived based on ammonia /hydrogen fuel mixture. Furthermore, by means of a chemical analysis tool named Rich-Quench-Lean, the behavior of combustion was investigated. Then, the results showed that the proposed model could significantly increase the thermal efficiency of overall system. The proposed humidified combustion of blending fuel displayed a low emissions within the combustion products, and a higher quantity of power was generated. Also, they showed that the NOx species emission was directly depended on oxygen and combustion temperature.

Besides, Bozo et al. [17] carried out another research on addition of steam to ammonia/hydrogen mixture in gas turbine system. They concluded that their proposed model could present the efficiency of cycle in same level as ordinary hydrocarbon based fuels. Furthermore, the steamed fuel mixture showed the stable condition of flame through the combustion, and the NOx emission declined through the steam injection into the ammonia based fuels.

Valera-Medina et al. [18] considered the ammonia/hydrogen fuel mixture inside a swirl combustor of a gas turbine system. Then, they examined volumetric ratio of 70/30 for ammonia/hydrogen fuel, by which stable flame was feasible. The results showed that the temperature of air at the inlet of compressor plays a key role in quantity of NOx emission. Hence, high temperatures at compressor entrance would degrade the flame development.

Aditya and Lim [19] conducted a research on diesel engines and ammonia homogenization. They modeled two injectors in order to improvement of injection process by which NOx emission was reduced.

Rahman et al. [20] evaluated the NOx generation through the ammonia oxidation. They showed that higher pressure leads to lower oxidation temperature as well as the lower NOx emission. In addition, they concluded that the re-burning of ammonia at a higher pressure will decrease the NOx emission by about 50%. Moreover, at the high

pressure oxy-combustion, nitrogen would be formed from NO.

Mohammadpour et al. [21] conducted a numerical study on MILD combustion of ammonia within a combustion chamber. They defined a reaction region and by means of two parameters named Lower wall temperature and air concentration, analyzed the thermal efficiency and NOx emission. They concluded that air concentration and lower wall temperature would affect the NOx and N_2O emission in different ways.

Ni and Zhao [22] inspected a procedure in order to reduction of NOx in ammonia fueled small-scale combustors. The operation was under the rich fuel mixture condition. In addition, the proposed process, i.e. utilizing a specific porous media, with high thermal conductivity could mitigate near to all quantity of released NO. Ni et al. [23] in another work studied the energy conversion performance and NOx emission value in an ammonia fueled small scale combustor. In rich region, they resulted that having a double rib in combustor could improve the thermal performance of the combustor, and about 50% NOx reduction would occur.

Han et al. [24] Conducted a study on a novel micro wavy combustor with ammonia/hydrogen fuel, which could extend the fuel flammability. They resulted that wavy combustor could improve the energy performance as well as a remarkable reduction of NOx emission. They also examined the effect of equivalence ratio on NOx emission and concluded that just over 20% reduction in NOx was experienced.

Ariemma et al. [25] studied the ammonia-methane combustion in a small combustor. They examined the NOx and other emission species as well as stability bounds of flame as a function of equivalence ratio. They proved that the ammonia/methane mixture develops the stability bounds better than a sole ammonia fueled system. However, they concluded that the ammonia/methane mixture results in higher NOx emission than in single ammonia fueled burner.

Matsumoto et al. [26] proposed a novel procedure to convert NOx species to ammonia in energy systems by which the toxic NOx compositions are converted to ammonia to reproduce and refuel within the cycle. The concept was practiced by means of a single stage process and in two dissimilar gas turbines with different temperatures. They examined the feasible arrangements NOx post-production which can undertake the proposed methodology.

Ma et al. [27] investigated the co-firing of ammonia/coil/biomass mixture within a swirl burner. Then, they realized that injecting the secondary air can mitigate the NOx emission. However, it was revealed slightly increase of unburnt carbon.

Ni et al. [28] conducted a computational study on reaction of ammonia-hydrogen. They investigated the reduction of NOx emission with a particular mechanism. They designed a double-end open combustor, and then analyzed the impacts of some parameters such as mass flow rate, hydrogen mass fraction and temperature. Furthermore, one chief outcome displayed that various temperatures of heat exchanger would increase the NOx emission.

Okafor et al. [29] modeled a small-scale gas turbine system fueled with ammonia-hydrogen. Then, they considered chemical and physical procedures in order to measure and regulate the NOx emission. They used the ammonia with heat fraction of 30% within the burner. They resulted that comparing the methane/ammonia and sole ammonia combustion in both the rich and lean regions, due to the upper flame speed, the former combustion releases lower quantity of NOx. Some additional investigations focused on NOx emission due to the ammonia combustion have presented in literatures [30], [31], [32], [33], [34].

Moreover, amid the issues respect with current study, the exhaust gas recirculation, EGR, is a significant subject between the vehicles by which major quantity of unburnt fuel containing pollution is re-combusted. This technology has absorbed the attention of scientists of energy systems field to employ and practice it to diminish the major CO2 and NOx emissions [35], [36], [37]. Lu et al. [38] Considered an oceanic diesel engine and carried out a computational analysis on injected exhaust gas recirculation, IEGR, for the proposed engine. They concluded that fuel-air mixture and the combustion performance would be improved by the proposed IEGR

system, also fuel consumption as well as NOx emission would be diminished using this equipment.

Resetar et al. [39] studied the impacts of eliminating the EGR system in a specified diesel vehicle. Accordingly, NOx emission were evaluated. They resulted that removing the EGR unit in such vehicle would threefold the NOx emission.

Hachem et al. [40] studied the EGR system in gas turbines using the first low and the exergetic approaches. The energetic analysis showed the slight negative effect of utilizing the EGR at full load operation, and an improvement in performance of the cycle in partial load operation.

Ditaranto et al. [41] proposed an innovative hydrogen plant using the EGR system. They showed the negative role of steam in hydrogen which leads in disorder of NOx emission. In addition, their work displayed a trivial improvement in performance of the cycle respect with the literature. Finally, regarding to the performance, they preferred the dry EGR system rather than a wet one.

Rosec et al. [42] analyzed the glycerol as a fuel and also evaluated the performance of EGR system in their research. They concluded that an external EGR equipment could mitigate the NOx emission. In addition, they analyzed the CO and NOx in certain EGR rates, and showed lower emissions in gas turbine system compared to the conventional diesel ones.

To the best of our recollection, no coupled series of ammonia and methane/ hydrogen Brayton cycles were reported among the literature. Hence, this work is a novel study to examine the results of such futuristic proposal. Accordingly, this study presents an innovative arrangement of ammonia Brayton cycle, which primarily aims to minimize the NOx emission as well as to maximize the power generation. However, as there is a reverse relation between increment of thermal efficiency and lower NOx emission, a group of chemical calculations should be considered prior to thermodynamic analysis. In addition, finding the optimum reactants' molar fractions of fuel-oxidizer leads us to receive a profound insight about the feasibility of proposed system. A media named equivalence ratio can resolve this problem, as finding the optimal molar fractions and the proper equivalence ratio sets our proposed system limited in a range of controlled values by which the higher feasible thermal efficiency regarding to the best design condition can be achieved. Also, another key parameter to sooth the high combustion temperature, is exhaust gas recirculation ratio by which a portion of combustion products are re-burned in boiler and then the residue product which is air without oxygen, i.e. almost nitrogen, returns into the cycle through the compressor. At the result, cold temperature nitrogen would be circulated in cycle to enforce the quality of combustion with a lower combustion temperature and an improvement in overall thermal efficiency of system.

On the other hand, the lateral cycles, i.e. steam Rankine cycle as well as methane/hydrogen Brayton cycle, are analyzed with the well-known thermodynamic approaches by which the states and the properties can be estimated. Hence, the specific work and thermal efficiency of each identical cycle would be determined.

Moreover, to measure the environmental approach, the various reactants and products are studied through the parametric study in which temperature and pressure besides the equivalence ratio are the most significant factors to present the quantity of the released carbon dioxide and NOx. The subsidiary objectives of this research are different, and can be multifold as follows:

- Depict an innovative integrated cycles of methane/hydrogen and steam Rankine into a topping cycle of ammonia Brayton.
- Evaluate the chemical and thermodynamic properties of the topping ammonia Brayton cycle as well as the bottoming methane/hydrogen Brayton cycle.
- Find the optimal EGR ratio consistence with optimal equivalency ratio of fuel mixture.
- Conduct the energy analysis to entire system.
- Conduct the parametric study over the entire proposed system.
- Discuss the optimum values and the chief characteristics of energetic and environmental analyses.

Nomenclature

a	Polynomial constant
$C_{p,i}$	specific heat capacity of the working fluid of state i, (kJ/kg.K)
dT	Temperature difference, (K)
h	Enthalpy (kJ/kg)
$\dot{m}$	mass flow rate (kg/s)
$\dot{n}_{air}$	molar flow of dry air fed to the gas turbine (mol/ s)
$\dot{n}_{EGR}$	molar flow of recirculated exhaust gas (mol/ s)
$\dot{Q}$	Heat rate, (kW)
R	Universal gas coefficient
s	Entropy, (kJ/kg.K)
T	Temperature, (K)
$\dot{W}$	power rate, (kW)
w	Specific work (kJ/kg)
$x_{i,j}$	molar fraction of component j in the working fluid of state i
$\Delta H^0_{f,j}$	standard enthalpy of formation of component j (Kj/mol)
η_{th}	Thermal efficiency (%)
φ	Equivalence ratio
P	product
R	reactant

Subscripts and Superscripts

chem	Chemical
i	state index
i	Inlet
j	Component index
o	Outlet
s	isentropic
sens	sensible

Abbreviations

TIT	Turbine inlet temperature
EGR	Exhaust gas recirculation
MW	Molecular weight
CV	Control volume
am	ammonia
st	steam
me	Methane
cogen	Cogeneration
gt	Gas turbine
ac	Air compressor
pum	pump
ATF_{stc}	stoichiometric air-to-fuel ratio
turb	turbine
cond	Condenser
cc	Combustion chamber
LHV	Lower heat value
HRSG	Heat recover steam generator

2. System description

Ammonia Brayton cycle employs ammonia as a promising carbon-free fuel. However, as the complete combustion of ammonia releases high temperatures, an integration of subsequent cycles is considered to use the maximum potential of power and the minimum amounts of NOx as well as carbon dioxide across the entire system. A schematic of the proposed NOx/Carbon-free cogeneration system is shown in Fig. . According to the figure, the topping ammonia-air cycle drives the sub-systems of steam Rankine and methane/hydrogen Brayton cycles. Each sub-system operates as follows:

2.1. Ammonia Brayton cycle

In search of the environmental power systems with high thermally efficient characteristics and plain arrangements, the ammonia Brayton cycle was selected from Keller et al. [43] as the driving cycle of the proposed system, shown in Fig. 1. Accordingly, it is assumed as the driving source in the proposed overall system and comprises the primary components of a basic Brayton system such as a compressor, a combustion chamber, and an expanding turbine.

Primarily, the necessary volume of air is taken into the air compressor under the reference conditions. However, this air is modified in the subsequent loops while the EGR unit is involved in circulating the mostly nitrogen-contained exhaust gases of the cycle. At the second state, a combustion chamber is a component at which the ammonia-air mixture is combusted. As the complete combustion of the ammonia fuel mixture releases a very high temperature in the order of 2000 K, employing the heat resistance materials would be crucial. The turbine is the third component in which the heat is converted to mechanical work by expanding high-temperature combustion products. Since the exhaust gas is an energy potent mass in conventional gas turbine systems, the exhaust gases are routed towards a Heat Recovery Steam Generator (HRSG), at which a portion of the remaining thermal energy is utilized as the heat source for bottoming cycles of steam Rankine and CH_4/H_2

Brayton cycles. Thermodynamic data for the ammonia cycle was employed from the study conducted by Keller et al. [43].

2.2. Steam Rankine cycle

As mentioned, the steam Rankine cycle is driven through the HRSG unit and utilizes the components of a regular Rankine cycle, as shown in Fig. 1. It also improves the power value into the ammonia cycle comparable with the conventional combined cycle power plants as a bottoming cycle. A backpressure steam turbine, a condenser, and a pump are constituted to create the steam Rankine cycle. Thermodynamic data for this cycle was brought from the National Institute of Standards and Technology (NIST) and Keller et al. [43], [44].

2.3. Methane/Hydrogen Brayton cycle

Conventional gas turbines take advantage of methane as a working fuel, and a carbon dioxide combination would be among its combustion products. Attempts to find resolutions for lessening this harmful emission have been the subject of different studies. One of the resolutions to diminish this environment-threatening issue is enhancing the hydrogen portion in the fuel mixture, which is one of the aims of this study. Therefore, a combination of methane and hydrogen is considered in the bottoming Brayton cycle by which the carbon-free products would be projected. In fact, the partial or total replacement of natural gas (i.e., CH4) with hydrogen-contained fuels is accompanied by a decrease in carbon dioxide emissions. In this study, a basic methane-air Brayton cycle is modeled from Tsatsaronits et al. [45], and a modification due to the manipulation in fuel composition is conducted to hire carbon-free exhaust gases. Also, the EGR unit is utilized to divide the appropriate portions of the exhaust air composition between the compressors of ammonia and methane-hydrogen Brayton cycles. The positive impact of the EGR on efficiency and the other parameters of the overall cycle is projected.

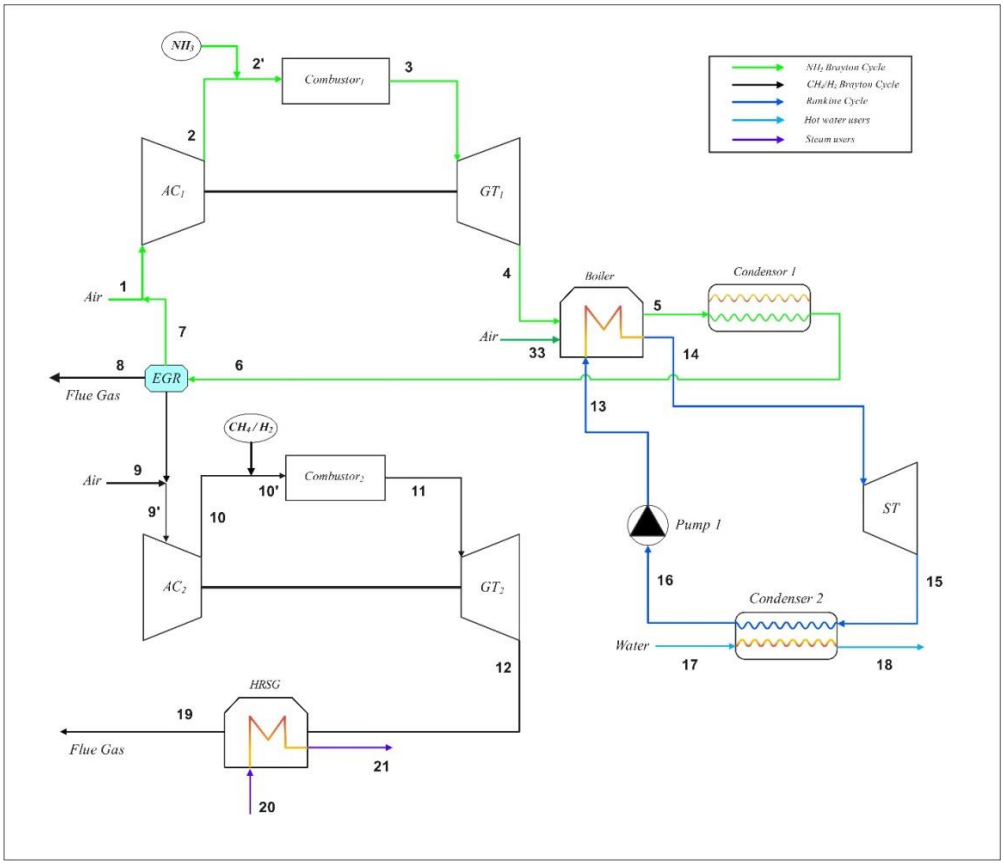

Fig. 1. Schematic of the proposed cogeneration system.

3. System model design

3.1. Assumptions and restrictions

Thermodynamic properties of the fuel mixture in the cycle states and the required modeling data of the proposed cogeneration system are derived from GASEQ and ANSYS CHEMKIN software. Furthermore, the performance of the proposed model is examined through the developed codes in EES (Engineering Equations Solver) software. However, to accurate analysis of the proposed system, some assumptions and restrictions are considered as follows [43], [46]:

- The proposed system operates in a steady-state condition.
- The control volumes of the process work adiabatically.
- Pressure drops in heat exchangers are neglected.
- Pump, turbines and compressors run with the specified isentropic efficiencies.
- Changes in kinetic and potential energies are neglected.

For a better understanding of thermodynamic characteristics in the three proposed cycles of ammonia, methane-hydrogen Brayton, and steam Rankine, the related Temperature-Entropy (T-S) diagrams are illustrated in Fig. 2. Besides, some rudimentary design data to measure the other thermodynamic parameters of the proposed system is listed in Table 1-3.

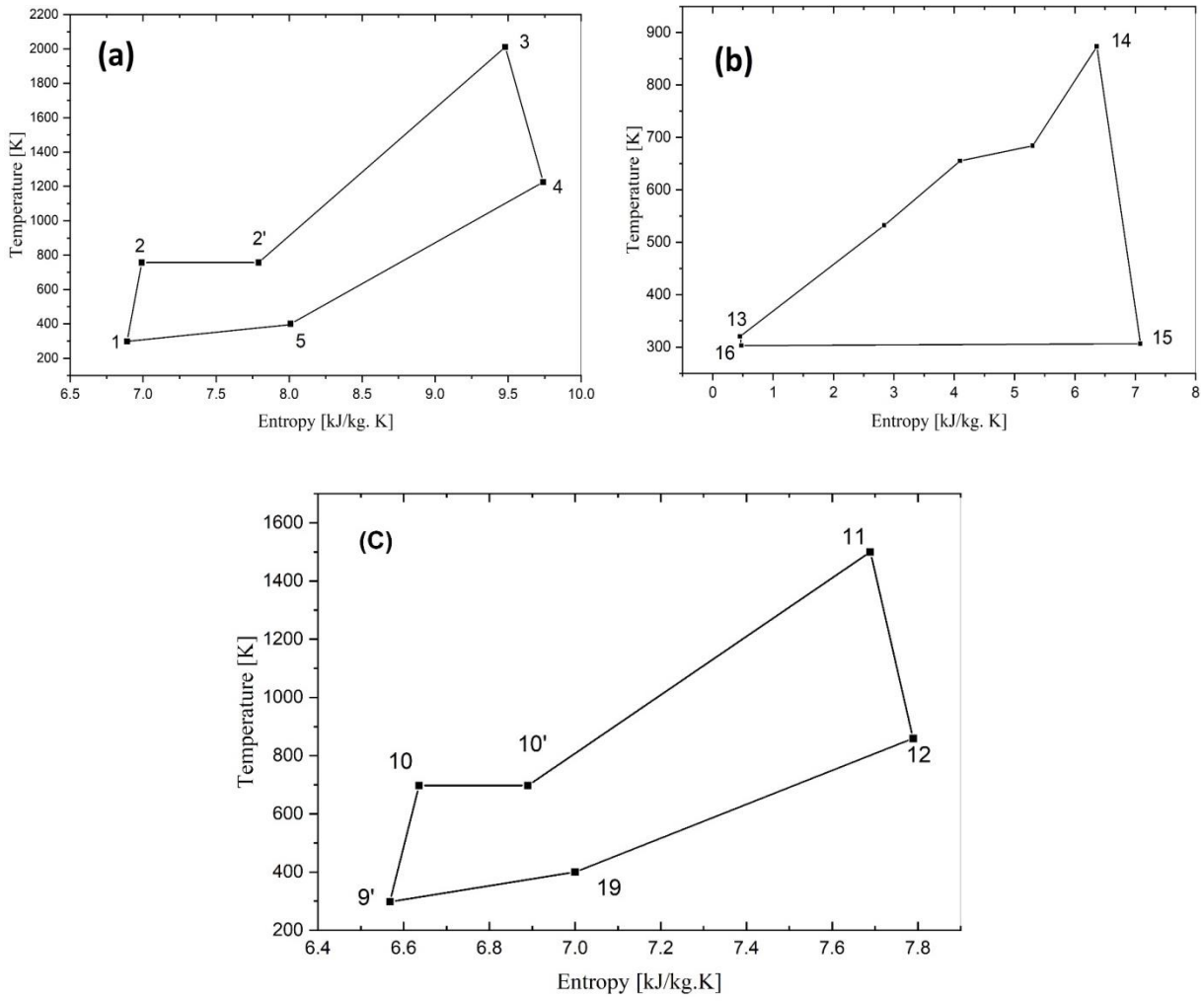

Fig. 2. T-S diagrams of the proposed (a) ammonia Brayton cycle, (b) steam Rankine cycle, (c) methane-hydrogen Brayton cycle.

Table 1. Required design parameters of the ammonia Brayton cycle **[43]**.

Parameters	Components	Value
Reference temperature, T_0 (K)		298.15
Reference pressure, P_0 (bar)		1
Pressure ratio	Compressor	20
TIT, T_3 (K)		2011
Isentropic Efficiency (%)	Compressor	85
Isentropic Efficiency (%)	Turbine	80
Thermal efficiency (%)	boiler	0.75
Outlet temperature, T_5 (K)	boiler	400
Equivalence ratio		1.2
EGR		0.4

Table 2. Required design parameters of the steam Rankine cycle **[43]**.

Parameters	Components	Value
inlet temperature, T_{14} (K)	Turbine	873
inlet pressure, P_{14} (bar)	Turbine	250
Outlet Pressure, P_{15} (bar)	Turbine	0.05
Specific net work, $w_{net,st}$(kJ/kg)	Turbine	1530

Table 3. Required design parameters of the methane/hydrogen Brayton cycle **[45]**.

Parameters	Components	Value
Reference temperature, T_0 (K)	-	298.15
Reference pressure, P_0 (bar)	-	1
Pressure ratio	Compressor	16
TIT, T_{11} (K)	turbine	1500

3.2. Methodology

Regarding the mentioned assumptions and restrictions, the thermodynamic properties of each constituent are assessed for the ammonia Brayton cycle and the bottoming cycles. In addition, to reutilize the high-temperature combustion products, the steam Rankine cycle is linked to the ammonia cycle. Furthermore, to establish of NOx free-carbon free cogeneration system, a methane-hydrogen Brayton cycle is augmented with some improvements. Consequently, the energy analysis is applied to inspect the thermodynamic performance of the individual systems. Then the remarkable features of each cycle and the entire system is discussed. A schematic of the procedure for calculation of the proposed cogeneration system is shown is Fig. 3.

3.2.1. Thermodynamic modeling

3.2.1.1. Enthalpy of mixtures

Heat capacity plays a significant role in the calculation of thermodynamic parameters of gas mixtures. Also, the relative polynomial constants calculate thermodynamics properties such as heat capacity and standard enthalpies of gas mixtures in different temperatures. These polynomial factors were driven from the database of ANSYS CHEMKIN software. Furthermore, it is noting that the following relative heat capacity coefficients are viable for all temperature sets using Eq.1, as follows [43]:

$$\frac{C_{p,j}(T)}{R}=a_{1,j}+a_{2,j}T+a_{3,j}T^2+a_{4,j}T^3+a_{5,j}T^4 \quad (1)$$

Where R denotes the universal gas coefficient. Since a real gas mixture contains numerous chemical species, particularly in combustion, many driven species through the chemical equilibrium in CHEMKIN are: H_2, O_2, N_2, H, O, OH, HO_2, H_2O, H_2O_2, NH_3, NO, N_2O and NO_2. Other species are neglected in calculations, as of their trivial particle concentrations. Moreover, the specific enthalpy of the i-*th* state includes the sensible and chemical enthalpies, which can be calculated by Eq. 2 [43]. In addition, some of the driven parameter values for different gasses are listed in Table 4.

$$h_i=h_{sens,i}+h_{chem,i}=\frac{1}{MW_i}\sum_j\int_{T_0}^{T}x_{i,j}\,C_{p,j}(T)dT+\frac{1}{MW_i}\sum_j x_{i,j}\,\Delta H^0_{f,j} \quad (2)$$

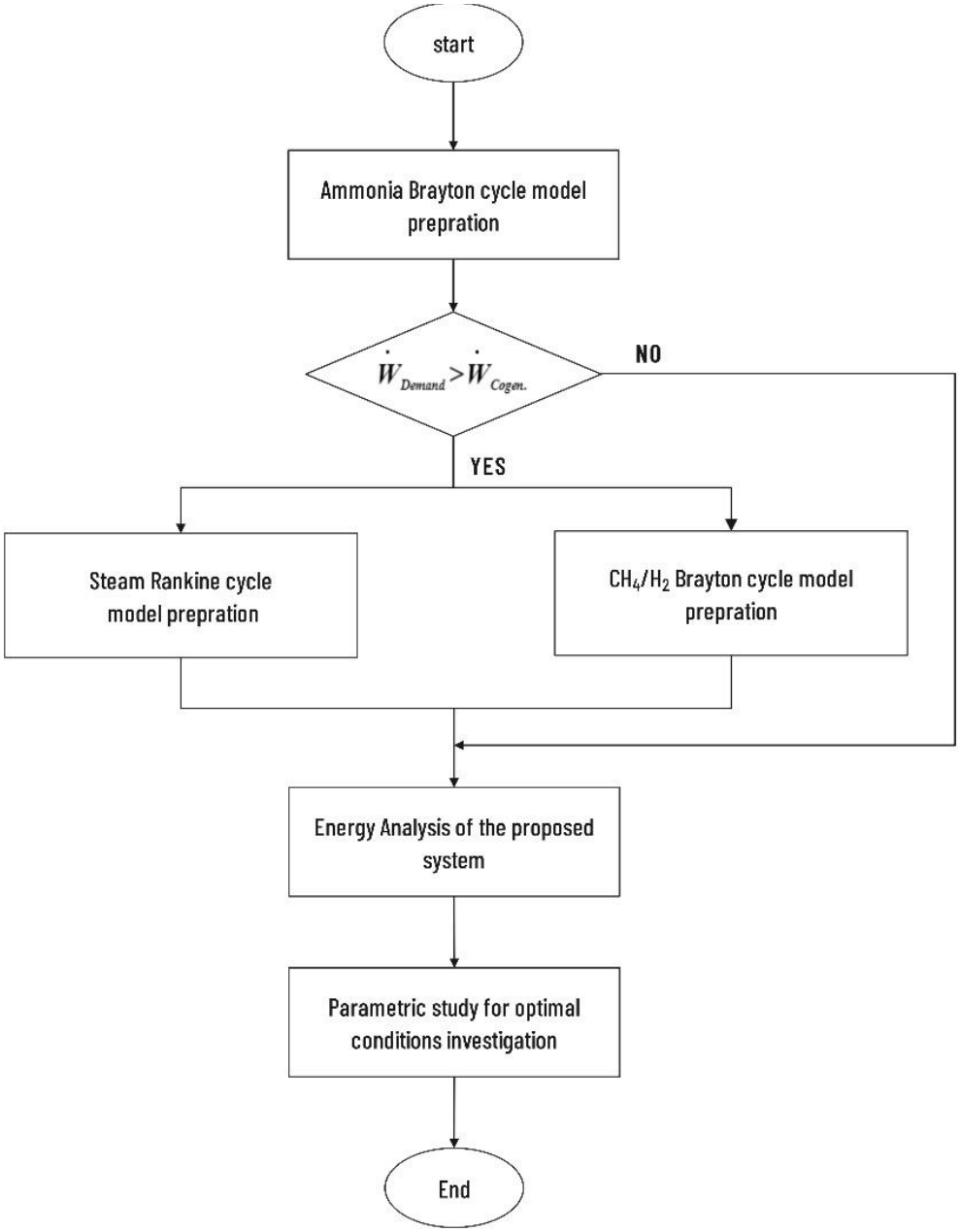

Fig. 3. Schematic of the procedure for calculation of the proposed cogeneration system.

Table 4. Some of the thermodynamic properties driven from ANSYS CHEMKIN.

Species	$H\ (300)$ $[kcal/mole]$	$S\ (300)$ $[cal/mole-K]$	$C_p(300)/R$	$C_p(400)/R$
H_2	-0.01	31.223	3.47	4.71
H_2O	-57.80	45.13	4.041	7.14
N_2	-0.01	45.79	3.50	4.51
NH_3	-10.98	46.07	4.29	9.90
NO	21.81	50.36	3.51	4.57
N_2O	19.50	52.58	4.66	7.73

3.2.1.2. Energy analysis

The various properties of a thermodynamic system at the input and output of any equipment can be defined using a set of governing equations among which the mass and the energy balances significantly affect the efficiency analysis of a thermodynamic system. Therefore, energy analysis of a system can be introduced under steady state and flow conditions as follows:

$$\sum m_{out} - \sum m_{in} = 0, \tag{3}$$

$$\sum (mX)_{out} - \sum (mX)_{in} = 0 \tag{4}$$

$$Q_{CV,out} - Q_{CV,in} + W_{CV,out} - W_{CV,in} - \sum (\dot{m}h)_{out} + \sum (\dot{m}h)_{in} = 0 \tag{5}$$

According to the mentioned input data shown in Tables 1–3, and utilizing the above equations, necessary parameters of the proposed cogeneration system can be resulted and shown in Table 5. In addition, some additional characteristics of the cycles can be determined through the equations as follows:

• **Overall cogeneration system Net Work**

$$W_{cogen} = W_{net,am} + W_{net,me} + W_{net,st} \tag{6}$$

• **Ammonia Brayton cycle Net Work**

$$W_{net,am} = W_{gt1} - W_{ac1} \tag{7}$$

• **Methane/Hydrogen Brayton cycle Net Work**

$$W_{net,me} = W_{gt2} - W_{ac2} \tag{8}$$

• **Steam Rankine cycle Net Work**

$$W_{net,st} = W_{st} - W_{pum1} \tag{9}$$

• **Ammonia Brayton cycle thermal efficiency**

$$\eta_{th,am} = \frac{W_{net,am}}{Q_{in,am}} \tag{10}$$

• **Methane/Hydrogen Brayton cycle thermal efficiency**

$$\eta_{th,me} = \frac{W_{net,me}}{Q_{in,me}} \tag{11}$$

• **Steam Rankine cycle thermal efficiency**

$$\eta_{th,st} = \frac{W_{net,st}}{\dot{m}_{st}(h_{14} - h_{13})} \tag{12}$$

• **Overall cogeneration system thermal efficiency**

$$\eta_{th,cogen} = \frac{W_{cogen}}{Q_{in,me} + Q_{in,am} + \dot{m}_{st}(h_{14} - h_{13})} \tag{13}$$

3.2.1.3. Exhaust Gas Recirculating system, EGR

The Exhaust Gas Recirculating system, comprised of N_2 and O_2, is proposed to progress the efficiency of both the ammonia and the methane Brayton cycles. This innovative system receives the air components and then divides them with a specific rate into the inlet of both air compressors while the fresh dry air is supplied to the cycle. The EGR also supplies the gas components in the reference temperature and pressure. The EGR ratio in the ammonia Brayton cycle is calculated by the fraction of the molar recirculated gas to fresh, dry air supplied into the cycle, as follows [43]:

$$EGR_{am} = \frac{\dot{n}_{EGR,am}}{\dot{n}_{AIR,am} + \dot{n}_{EGR,am}} \tag{14}$$

Also, the portion of EGR supplied into the methane cycle can be derived as below:

$$EGR_{me} = \frac{\dot{n}_{EGR,me}}{\dot{n}_{AIR,me} + \dot{n}_{EGR,me}} \tag{15}$$

3.2.1.4. Mass flow rate and specific net work

The mass flow rate of the flows passing through the compressor and turbine can be denoted by $\dot{m}_1$ and $\dot{m}_4$, respectively, while those for the methane cycle are indicated by $\dot{m}_9$ and $\dot{m}_{12}$. The ratio of air to fuel mass flow (ATF) for a stoichiometric supply of air is defined as:

$$ATF_{stoic} = \frac{\varphi m_{air}}{m_{fuel}} \tag{16}$$

The equivalence ratio value, φ, for ammonia and methane/hydrogen are 1.2 and ~1, respectively. Moreover, ATF_{stoic} value depends directly on the heat value of fuel mixtures, e.g., NH_3 with a lower heat value (LHV_{NH3}=2.64 MJ/kg) holds the small value of 6.05, which is not comparable to those of methane (LHV_{CH4}=50 MJ/kg) and hydrogen (LHV_{H2}=120 MJ/kg). The equation is applied

for both ammonia and methane Brayton cycles. Hence, the mass flow rates in inlets and outlets of both gas turbines can be defined as follows:

$$m_1 = m_{air,am} + m_{EGR,am} \quad (17)$$

$$m_4 = m_1 + m_{NH3} \quad (18)$$

$$m_9 = m_{air,me} + m_{EGR,me} \quad (19)$$

$$m_{12} = m_9 + m_{CH4/H2} \quad (20)$$

Therefore, specific net work of the gas turbines regarding the above mass flow rates can be defined as follows:

$$w_{gt,am} = w_{GT1} - w_{AC1} = (h_3 - h_4) - (h_2 - h_1)\frac{m_1}{m_4} \quad (21)$$

$$w_{gt,me} = w_{GT2} - w_{AC2} = (h_{11} - h_{12}) - (h_{10} - h_9)\frac{m_9}{m_{12}} \quad (22)$$

Also, the above Eqs. (21) and (22) can be improved with the substitution of Eqs. (16-20):

$$w_{gt,am} = w_{GT1} - w_{AC1} = (h_3 - h_4) - (h_2 - h_1)\frac{1 + \frac{m_{EGR,am}}{m_{air,am}}}{1 + \frac{m_{EGR,am}}{m_{air,am}} + \frac{\varphi_{am}}{ATF_{stoic,am}}} \quad (23)$$

$$w_{gt,me} = w_{GT2} - w_{AC2} = (h_{11} - h_{12}) - (h_{10} - h_9)\frac{1 + \frac{m_{EGR,me}}{m_{air,me}}}{1 + \frac{m_{EGR,me}}{m_{air,me}} + \frac{\varphi_{me}}{ATF_{stoic,me}}} \quad (24)$$

As ammonia combustion contains an unburnt hydrogen volume, due to the under-rich condition through the turbine expansion, the exhausted gas at the turbine outlet should be re-burnt so that the final species could be free of any hydrogen. For this reason, the high-temperature products need an amount of oxygen to re-combustion. At this stage of the process, if the unburnt hydrogen is more than volumetric 1%, the HRSG unit calls for a specified volume of fresh air. This secondary combustion takes place under adiabatic conditions, and consequently the hot exhaust gases flow into the HRSG to exchange the heat with the cold water stream to drive the steam Rankine cycle, which is formulated in the following section.

After transferring the heat, the leaving gas, which is now comprised of chiefly nitrogen and little oxygen, flows into the EGR system. The temperature of the gas at this state is about 400 K (T_5). Fig. 4 shows the algorithm of calculating the various thermodynamic parameters required in the energy analysis of the system.

3.2.1.5. Energy analysis in steam Rankine cycle

The bottoming Steam Rankine cycle is constituted to utilize the high-temperature combustion products of the gas turbine system before leaving through the stack. The HRSG system drives the steam Rankine cycle, and an additional amount of electricity is generated. Here, the Rankine cycle is modeled with simple components shown in Fig 1, and the thermodynamic properties of the states are calculated regarding the primary data listed in Table 2. High-pressure steam flows in and drives the turbine at state 14, and temperature and pressure are assumed to operate at 873 K and 250 bar, respectively. Significant thermodynamic parameters stem from energy balance among the various cycle states are calculated according to NIST steam data as listed in Table 5 [43].

Hence, the net specific work of the steam turbine is calculated as follows:

$$w_{net,st} = w_{st} - w_{pum1} = (h_{14} - h_{15}) - (h_{13} - h_{16}) \quad (25)$$

In addition, to calculate the mass flow rate of the steam, the energy balance through the HRSG is carried out as follows:

$$m_{gas,HRSG}(h''_4 - h_5)\eta_{HRSG} = m_{steam}(h_{14} - h_{13}) \quad (26)$$

Where η_{HRSG} refers to the thermal efficiency of the HRSG with a constant value of 0.75. In addition, $\dot{m}_{gas,HRSG}$ is defined as the sum of the mass flow rate of exhaust gas passing through the gas turbine and the mass flow rate of the added air for complete combustion of remained H_2 particles in the HRSG unit. Table 6 presents the energy balance and the auxiliary equations of the proposed system.

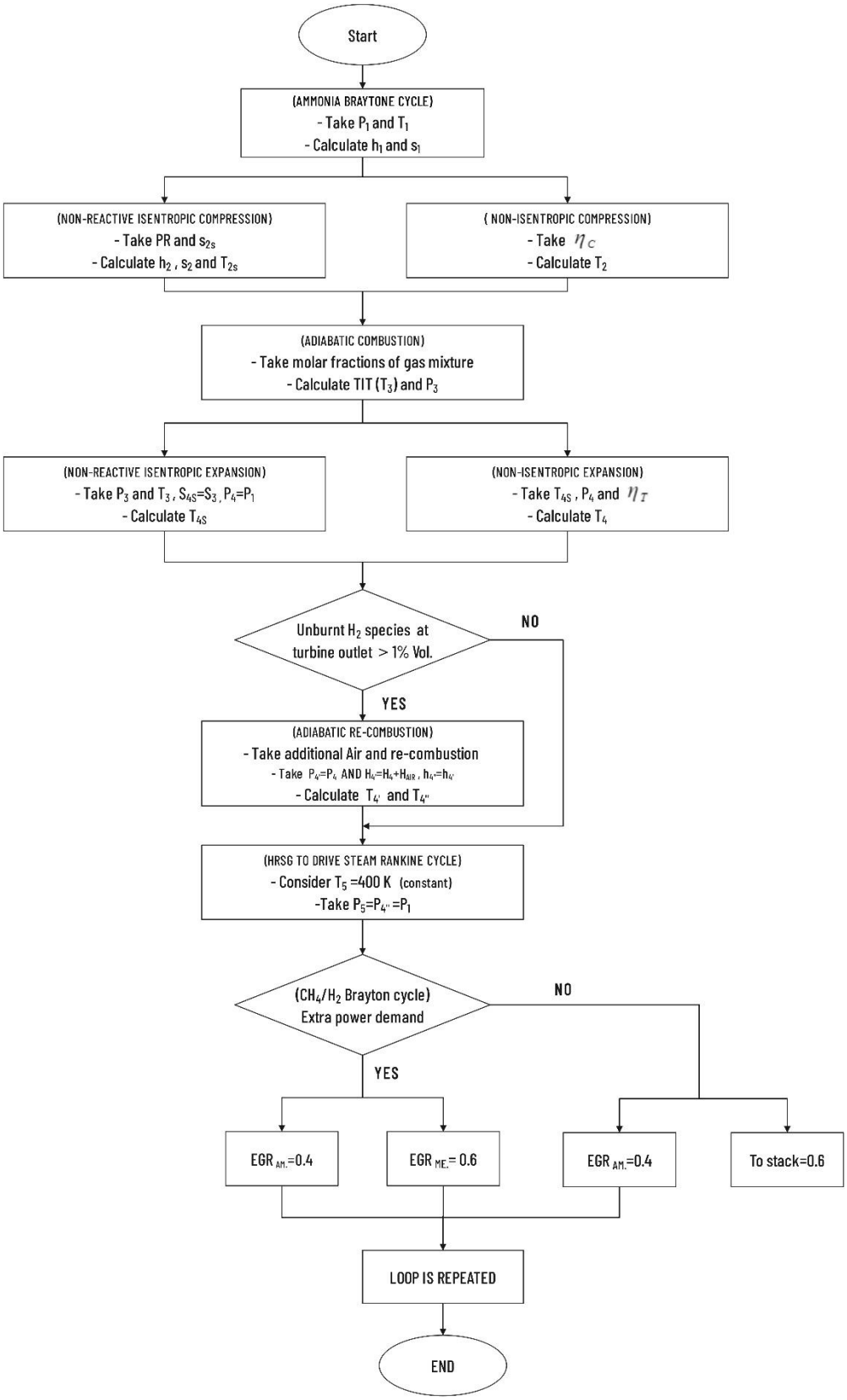

Fig. 4. Algorithm for calculation of thermodynamic properties of the states.

Table 5. Thermodynamic properties for different states of the proposed Brayton cycles and Steam Rankine cycle.

State	Temperature [K]	Pressure [bar]	Enthalpy [kJ/kg]	Entropy [kJ/kgK]
Ammonia Brayton cycle (ϕ= 1.2, EGR =0.4 and PR =20)				
1	298.15	1	0.04	6.89
2	757	20	482.6	7
2’	757	20	229.8	7.8
3	2011	20	229.8	9.5
4	1225.3	1	-982.45	9.75
5	400	1	-2244	8
Merthane/Hydrogen Brayton cycle (ϕ= 1, PR =16)				
9’	298.15	1.013	121.8	6.568
10	698	16.71	541.7	6.636
10’	698	18	580	6.89
11	1500	15.2	1725	7.689
12	859	1.025	827.6	7.789
Steam Rankine cycle				
13	873.15	250	3493.5	6.36
14	306	0.05	1398	6.36
15	306	0.05	138	0.48
16	307	250	163.5	0.48

Table 6. Energy balance and auxiliary equations of the proposed system.

Component	Energy equation	Auxiliary equation (I)	Auxiliary equation (II)
(a) NH_3 Brayton cycle			
Compressor (I)	$w_{comp,I} = h_{in} - h_{out,s}$	$h_2 = h_1 - \frac{h_1 - h_{2,s}}{\eta_{comp}}$	
Combustion chamber (I)	$q_{cc,I} = h_{out} - h_{in}$	$\dot{m}_{2'} = \dot{m}_3$	
Gas turbine (I)	$w_{turb,I} = (h_{in} - h_{out})\eta_{turb}$	$h_4 = h_3 - (h_3 - h_4)\eta_{turb}$	
Condenser (I)	$q_{cond,I} = h_{in} - h_{out}$	$(h_5 - h_6) = (h_{out,c} - h_{in,c})$	
Re-combustion unit	$q_{rc} = h_{out} - h_{in}$	$\dot{m}_4 + \dot{m}_{33} = \dot{m}_5$	
HRSG (I)	$q_{HRSG,I} = h_{in} - h_{out}$	$(h_4 - h_5) = (h_{out,c} - h_{in,c})$	
EGR_{am}	$EGR_{am} = 0.4 * EGR$	$\dot{m}_6 = \dot{m}_7 + \dot{m}_8 + \dot{m}_9$	$\dot{m}_1 = \dot{m}_{air,1} + \dot{m}_7$
(b) CH_4/H_2 Brayton cycle			
Compressor (II)	$w_{comp,II} = h_{in} - h_{out,s}$	$h_{out} = h_{in} - \frac{h_{in} - h_{out,s}}{\eta_{comp}}$	
Combustion chamber (II)	$q_{cc.II} = h_{out} - h_{in}$	$\dot{m}_{10'} = \dot{m}_{11}$	
Gas turbine (II)	$w_{turb,II} = (h_{in} - h_{out})\eta_{turb}$	$h_{12} = h_{11} - (h_{11} - h_{12})\eta_{turb}$	
HRSG (II)	$q_{HRSG.II} = h_{in} - h_{out}$	$(h_{12} - h_{19}) = (h_{21} - h_{20})$	
EGR_{me}	$EGR_{me} = 1 - EGR_{am}$	$\dot{m}_{9'} = \dot{m}_{air,9} + \dot{m}_9$	
(c) Steam Rankine cycle			
HRSG (I)	$q_{HRSG,I} = h_{in} - h_{out}$	$(h_{14} - h_{13}) = (h_4 - h_5)$	
Steam turbine	$w_{ST} = (h_{in} - h_{out})\eta_{turb}$	$h_{15} = h_{14} - (h_{14} - h_{15})\eta_{turb}$	
Condenser (II)	$q_{cond,II} = h_{in} - h_{out}$	$(h_5 - h_6) = (h_{out,c} - h_{in,c})$	
Pump	$w_{pump} = h_{out} - h_{in}$	$\eta_{ise,p} = \frac{h_{13,s} - h_{16}}{h_{13} - h_{16}}$	

Table 7. Validating data from the thermodynamic calculation results between topping Ammonia Brayton cycle and steam Rankine cycle in present study with those of Keller et al.

Parameter	Present study	Literature
Equivalence ratio	1.2	1.2
Pressure ratio	20	20
EGR	0.4	0-0.6
Isentropic efficiency of compressor	0.85	0.85
Isentropic efficiency of turbine	0.8	0.8
TIT(K)	2011	2000
Ammonia cycle thermal efficiency	0.6381	0.632
Boiler efficiency	0.75	0.75
ATF_{stoich}	6.05	6.05
Boiler outlet temperature (K)	450	400
Steam turbine inlet pressure (bar)	250	250
Steam turbine inlet temperature (K)	873	873
Steam turbine thermal efficiency	0.256	0.252

Table 8. Validating data from the thermodynamic calculation results between methane/hydrogen Brayton cycle in present study with those of Tsatsaronis and Morosuk.

Parameter	Present study	Literature
Pressure ratio	16	16.7
Isentropic efficiency of compressor	0.85	0.85
Isentropic efficiency of turbine	0.8	0.8
TIT(K)	1500	1500
Air mass flow rate (kg/s)	200	247.8
Fuel mass flow rate (kg/s)	5	5.489
Fuel inlet pressure (bar)	16	18
Methane cycle thermal efficiency	0.365	0.363
Specific work of gas turbine(kJ/kg)	897	881

4. Results and discussion

4.1. Model verification and comparison

4.1.1. Model verification

In this section, in order to validation of accuracy of the current work, a comparative analysis between the present work and the reference literatures are conducted. Thus, the results from Ammonia Brayton cycle combined with steam Rankine cycle in present study are compared and also discussed.

Therefore, for the topping cycle of the overall system, i.e. Ammonia Brayton cycle, input and output data through the chemical as well as thermodynamic analyses are calculated and also are compared with those of Keller et al. [43].

Similarly, the input and output data from the CH4/H2 Brayton cycle, which is augmented to topping cycle through EGR unit, are calculated, and then are compared with those of Tsatsaronis and Morosuk (2012), with fixed input factors. Accordingly, as can be seen in Tables 7 and 8, achieved results are utmost in consistent with those of the mentioned literatures.

4.1.2. Model comparison

In this part, three proposals including ammonia Brayton cycle as topping system, steam Rankine cycle and methane Brayton cycle, with thermodynamic data displayed in Table 5, are computed by the programing in EES software, then are compared with those of the literatures.

The foundational phase is to analysis the results of ammonia Brayton cycle in the present study with by those of Keller et al. [43] using the chemical and thermodynamic approaches. In this literature, to enliven the concept of carbon-free energy systems, Keller et al. devised an ammonia Brayton cycle that was ran as a topping system for a steam

Rankine cycle to constitute a combined power plant. Ammonia as working fluid of the proposed cycle operated the cycle to yield the results, which is compared with the model in the current study shown in Table 7. Therefore, nearly same thermal efficiencies were generated among the ammonia and steam cycle through the both researches. Accordingly, 0.009% more thermal efficiency of ammonia Brayton cycle was calculated in the present research, due to the higher TIT amount by 2011K. In addition, 1.58% more thermal efficiency of steam Rankine cycle was logged than that of literature. That was owing to the greater boiler outlet temperature, i.e. 450 K. Furthermore, while Keller et al. employed various EGR ratios in their work, this study used just quantity of 0.4, as it was calculated as the optimum value in consistence with equivalence ratio of 1.2. Moreover, the other thermodynamic parameter was completely in consistence with those of Keller et al.

Next step is to employ the methane Brayton cycle as the bottoming cycle of proposed system, which receives the advantages of the topping cycle through the EGR unit. By adding a portion of the cold temperature EGR, which contains the air without oxygen, lower combustion temperature and improvement in performance of the cycle will be resulted. The origin of current study is based on a study by Tsatsaronis and Morosuk [45], and the results are modeled and simulated through chemical and thermodynamic approaches.

Therefore, methane as working fluid of this bottoming cycle runs the cycle and the results from the thermodynamic calculation of cycle is compared with the programing output data in the current study shown in Table 8.

Hence, while the literature showed 36.3% thermal efficiency, the simulation results in current study yielded 0.55% higher value by 36.5%. In addition, the isentropic efficacies of compressor and turbine in both the scenarios were in consistence. Pressure ratio of compressor in current study is 0.7 lesser than in that of Tsatsaronis and Morosuk. Moreover, as TIT in both the scenarios were identical and also in consistent with value 1500 K in literature, the air mass flow rate was decreased about 20% down to 200 kg/s. Likewise, methane mass flow rate in present study showed 8.9% lower than literature. Moreover, specific work of the cycle was logged by 897 kJ/kg, which was 1.8% higher than results of Tsatsaronis and Morosuk. Other parameters in both of the researches were in consistency.

4.2. Parametric study

In this section, initially the various main thermodynamic parameters, including the reactant temperature, reactant molar fractions, equivalence ration of ammonia and methane cycles, EGR value and combustion chamber inlet pressures in both the ammonia and methane cycle are selected. Subsequently, the effect of variation of these parameters on the unfixed value of the different thermodynamic measures in the proposed system, such as thermal efficiency, net output power of the overall system, net output power of individual cycles, products temperatures, molar fraction of product compositions, is studied.

4.2.1. The impact of ammonia molar fraction on combustion products temperature

Influence of variation of ammonia molar fraction on the equivalence ratio and products temperature of the combustion chamber of ammonia Brayton cycle is investigated, as shown in Fig. 5.

According to the figure, an escalation in NH_3 molar fraction is resulted in rise of the equivalence ratio of the ammonia Brayton cycle, thus the fuel composition would be richer. This is principally due to the progress in share of the ammonia as the fuel in combustion chamber. On the other hand, products temperature revealed an oscillation in which the extreme value of 2250 K occurs in NH_3 molar fraction of 0.2. Although the starting point shows a lower temperature of 1300K in molar fraction of 0.1, the minimum products temperature is logged in the ending NH_3 molar fraction of 0.5 by 1100K. As a result, regarding to the calculated thermal efficiency, a decrease in thermal efficacy of ammonia Brayton cycle appears between 0.2 and 0.5 of NH_3 molar fraction, while the calculated optimum thermal efficiency is determined by 75% in the molar fraction of 0.25 for ammonia.

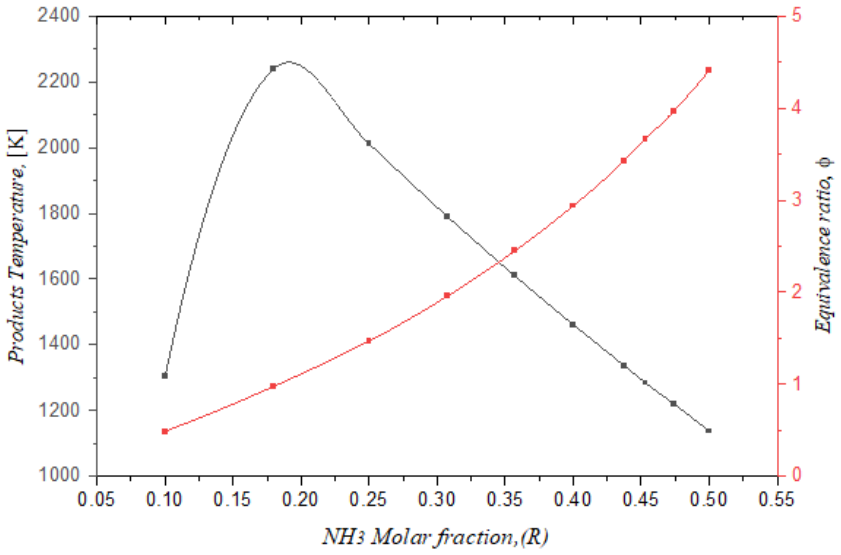

Fig.5. the impact of ammonia molar fraction on products temperature

4.2.2. The impact of ammonia molar fraction on molar fractions of combustion products.

Influence of variation of ammonia molar fraction on the various produced components at outlet of the combustion chamber of ammonia Brayton cycle is investigated, as shown in Fig. 6.

According to the figure, a sharp growth in H_2 molar fraction is resulted with increase of the ammonia molar fraction of the ammonia Brayton cycle, thus the hydrogen composition would be yield as a combustion product. This is chiefly because of the break down in reactive ammonia at the presence of air in combustion chamber. The minimum produced hydrogen can be seen while the ammonia molar fraction in reaction zone is about 0.1, while the utmost value of hydrogen, by 0.4, is yielded once the reactive ammonia molar fraction is projected by 0.5. Also, H2O appears as another combustion product due to the mixture of ammonia and air as the reactive gases. As can be seen, there is a decreasing trend of H2O production, which means that growth in the reactive ammonia, i.e. by 0.5, would lead in the least amount of gaseous water by just under 0.125. However, the maximum producing gaseous H2O, about 0.26 molar fraction, is cited once the reactive ammonia is recorded by 0.2 of reaction molar fraction. This shows that the more reactive NH3, the less reactive air, which means the water is produced fewer with decrease in value of reactive oxygen.

On the left hand, produced nitrogen and NO components show similar decreasing trend by increase in reactive ammonia. As can be seen, N2, as the major component of the combustion products, is decreased to final value of 0.475 at the presence of 0.5 reactive ammonia molar fraction. This can be due to decrease in reactive nitrogen portion. Nitrogen oxide, NO, as a toxic combustion product shows a sharp fall to amount of zero by presence of 0.18 reactive ammonia. This can be counted as a positive point in which environmental concerns of ammonia usage as a fuel is announced by the experts. In conclusion, this graph shows the optimal reactive ammonia towards achieving the lowest NO and the highest H2 among the combustion products.

4.2.3. The impact of equivalence ratio on temperature and molar fraction of combustion products

Influence of variation of equivalence ratio on temperature and molar fraction of combustion products in ammonia Brayton cycle is studied, as shown in Fig. 7. According to the figure, there is a sharp escalation in products temperature as well as H_2O molar fraction is shown with increase of the equivalence ration in between $0.7 \leq \varphi \leq 1$, but once placing the fuel mixture in rich zone, i.e. after $\varphi = 1$, a

smooth decreasing trend takes place. The optimal equivalence ratio, $\varphi = 1.2$, is placed in decreasing zone, where H2O molar fraction is 0.245, and combustion products temperature is about 2150 K. Variation of φ holds completely different trends on molar fraction of NO and H2. While NO molar fraction shows the utmost value, about 0.09, in $\varphi = 0.7$, its value falls down to zero by increase in value of φ and also shifting from lean zone to rich zone. Hence, the minimum NO molar fraction rests in zero in rich zone, i.e. $\varphi \leq 1$, which means the complete burning of N2 and O2 contents.

H2 shows to track entirely different trend than NO, as can be seen on figure. Growth of φ and shifting the mixture zone from lean to rich leads to increase in H2 value in reacting gases, due to the increase in hydrogen portion among the pre-combustion air-ammonia mixture. Hence, the minimum value of H2, i.e. zero, is placed in $0.7 \leq \varphi \leq 1$. Furthermore, with change in ammonia fraction and increase in reactive hydrogen, H2 molar fraction in combustion products would rise sharply so that in $\varphi = 1.4$, hydrogen value would grow to about 0.1.

Finally, variation of φ due to increase in ammonia and decrease in air in combustion process leads to increase of combustion products temperature, decrease and remove of NO from combustion products, and also increase in H2 molar fraction stem from a higher reactive NH_3.

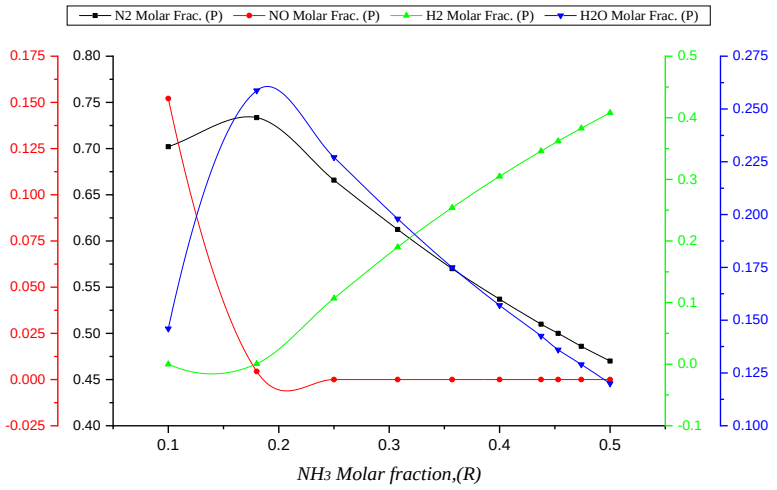

Fig.6. The impact of ammonia molar fraction on molar fractions of combustion products.

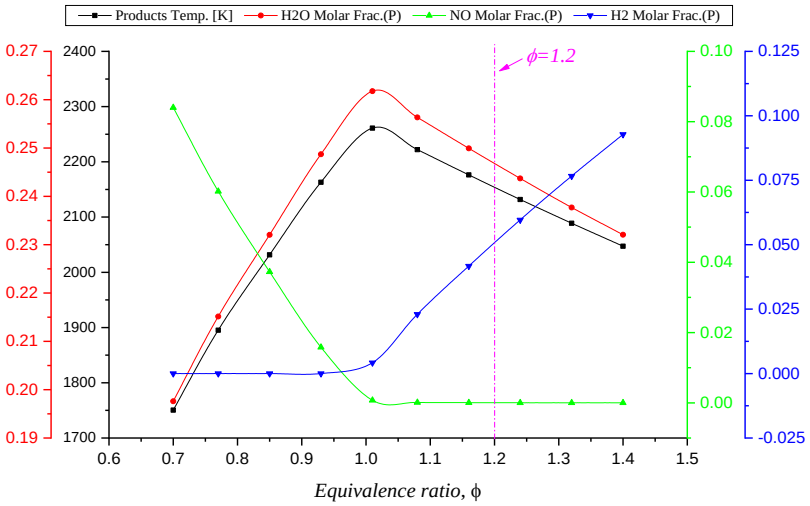

Fig.7. The impact of equivalence ratio on temperature and molar fraction of combustion products.

4.2.4. The impact of equivalence ratio on $NO_{(P)}$ and $NH_{3(R)}$ molar fractions.

Impact of changes in equivalence ratio (φ) on molar fractions of reactant ammonia, $NH_{3(R)}$, and Nitrogen monoxide, $NO_{(P)}$ among the combustion products in ammonia Brayton cycle are studied, as shown in Fig. 8. According to the figure, Increase of ammonia in fuel-air mixture inside the combustion chamber leads to a rich combination and, consequently, the equivalence ratio is increased.

As can be seen, the lowest value of φ is placed where the reactant ammonia, $NH_{3(R)}$, positioned by 0.14. Meanwhile, the increase in concentration of $NH_{3(R)}$ by 0.24 leads in progress of rich fuel mixture, i.e. $\varphi = 1.4$. Also, in the optimum equivalence ratio, i.e. $\varphi = 1.2$, the most suitable amount $NH_{3(R)}$ is recorded by 0.215. in this optimal point, the lowest amount of NO_X is shown by zero, which means that the fuel mixture is fully-environmental. Also, the $NO_{(p)}$ molar fraction graph among the combustion products reveals that the interval of lean equivalence ratio, i.e. $0.7 \leq \varphi \leq 1$, holds a declining trend of $NO_{(p)}$ from the utmost value of 0.08 to zero. Hence, it is concluded that the free-NO zone is taken place in rich fuel zone, i.e. $\varphi \geq 1$.

4.2.5. The impact of reactants temperature of CH4/H2 cycle on products properties.

The impact of changes in temperature of reactants in bottoming CH4/H2 Brayton cycle on the properties of combustion products are studied, as shown in Fig. 9. According to this figure, Increase in temperature of reactants leads directly in growth of products temperature. In other words, the lowest reactants temperature, 400 K, results in the bottom point of 1700 K, and the linear increase in temperature of reactants mixture by 1000 K would raise up to the point of 2200K, while the convenient methane-fueled Brayton cycle yields the operating temperature of 1300 K inside the combustion chamber.

On the other hand, a general decreasing trend can be seen over the all three molar fraction graphs. Nitrogen, N2, as the major combustion product retains the prime portion of molar fractions of mixture within 0.67. Increasing the temperature of combustion of CH4/H2-air from 400 K to 1000K leads in a slight decrease of molar fractions. Although hydrogen, H2, holds tiny amount of combustion products, interval of 0.099, it follows a slight decreasing trend similarly. In addition, concentration of gaseous H2O would be decreased by increasing the reactants temperature from 0.2299 to 0.2295.

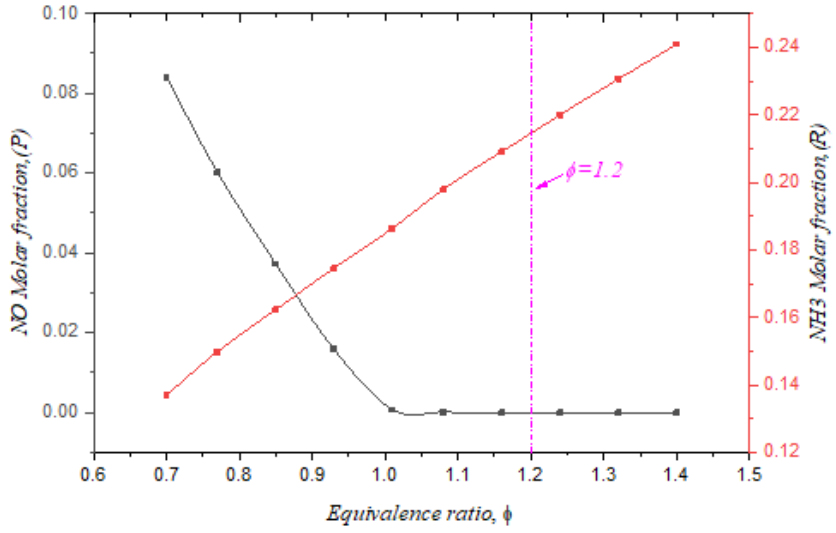

Fig.8. The impact of equivalence ratio on NO(P) and NH_3(R) molar fractions.

4.2.6. The impact of variation of equivalence ratio on products temperature of CH4 and CH4/H2 cycles.

The effect of variation of equivalence ratio on products temperature of CH4 and CH4/H2 cycles are studied, as depicted in Fig. 10. According to this figure, increase in equivalence ratio of fuel mixture shows same trends of products temperature in both CH4 and CH4/H2 cycles. Accordingly, at $\varphi = 0.5$ temperature of products of CH4 and CH4/H2 cycles are 1700K and 1150K, respectively. Although at the last point of $\varphi = 2.5$, temperature of CH4/H2 cycle is more than CH4 one by 1900K and 1500K, respectively.

The optimal equivalence ratio point, i.e. $\varphi = 1$, leads in the utmost products temperature in both the CH4 and CH4/H2 cycles by 2420K and 2150K, respectively. It is worth noting that the lesser products temperature in CH4/H2 cycle is an advantage where durability and safety of equipment components matter.

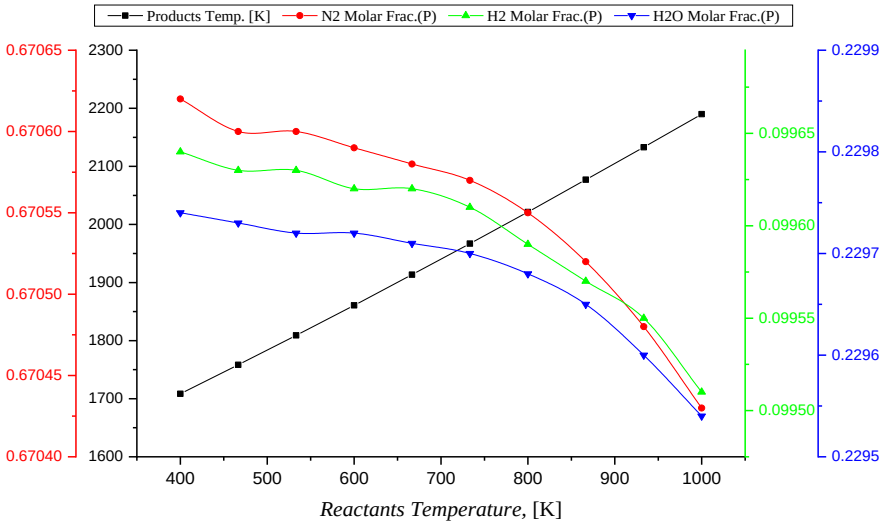

Fig.9. The impact of reactants temperature of CH4/H2 cycle on products properties.

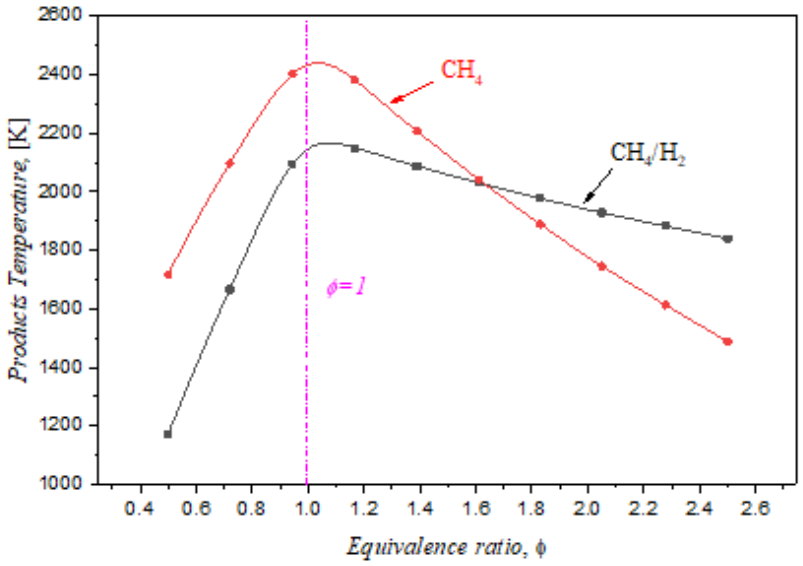

Fig.10. The impact of variation of equivalence ratio on products temperature of CH4 and CH4/H2 cycles.

4.2.7. The impact of variation of equivalence ratio on CO2 molar fraction of products in CH4 and CH4/H2 cycles.

The influence of variation of equivalence ratio on CO2 molar fraction of products in CH4 and CH4/H2 cycles are studied, as depicted in Fig. 11. According to this figure, there are dissimilar behavior through the mole fraction of carbon dioxide in the two lean and rich regions of the mentioned cycles. As can be seen, in the lean region of methane Brayton cycle, i.e. $0.4\leq\varphi\leq1$, the quantity of carbon dioxide increases from 0.05 of mole fraction up to 0.085, while in the region of rich mixture, i.e. $1\leq\varphi\leq2.5$, this molar fraction decreases from 0.08 to 0.02.

On the other hand, due to the presence of an excess amount of hydrogen blended with methane, through the Brayton CH4/H2 cycle, the portion of carbon is diminished. Therefore, molar fraction of carbon dioxide in the lean region, i.e. $\varphi < 1$, is less than 0.01. Although, CO2 molar fraction among the rich region, $1\leq\varphi\leq2.5$, stands on zero.

At the optimal point of the graphs, i.e. $\varphi=1$, the molar fraction of carbon dioxide in two CH4/H2 and CH4 cycles are 0.007 and 0.082, respectively. Therefore, due to the slight amount of produced carbon dioxide in CH4/H2 cycle scenario, it is a perfect scenario from environmental point of view.

4.2.8. The impact of reactants temperature of CH4 and CH4/H2 cycles on molar fraction of combustion products.

The effects of change in reactants temperature of CH4 and CH4/H2 cycles on the molar fraction of combustion products in the optimal equivalence ratio, i.e. $\varphi=1$, are analyzed, as shown in Fig. 12. According to this figure, carbon dioxide chiefly takes the notable share of combustion products in CH4 and CH4/H2 scenarios. Therefore, combustion of methane-air mixture yields more Carbone dioxide by 0.09 molar fraction at 300K, however, increasing the reactants temperature up to 700K results in a slight decrease of molar fraction to 0.085. Unlikely, due to the presence of hydrogen in CH4/H2 scenario, and decrease of reactant carbon in methane, release of CO2 in this scenario decreases remarkably in which a constant value of 0.04 CO2 molar fraction is shown along the curve. This means that CH4/H2 cycle is a near zero carbon free scenario.

In other hand, CH4/H2 cycle holds no amount of CO and NO, however, CH4 scenario shows a bit more quantities of CO and NO by 0.01 and 0.0025, respectively, at maximum temperature spot of 700K. Consequently, the given data at optimum equivalence ratio, i.e. $\varphi=1$, depicts the encouraging impact of hydrogen amid the fuel blending, and also it represents CH4/H2 Brayton cycle as the environmental-friend scenario.

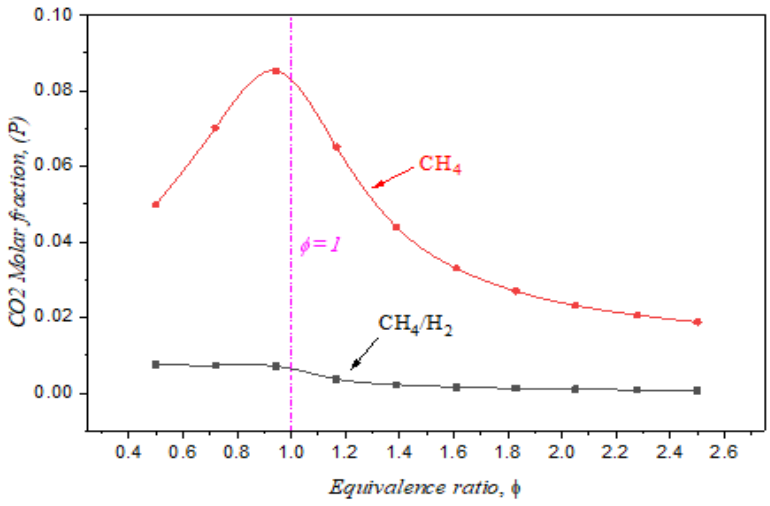

Fig.11. the impact of variation of equivalence ratio on CO2 molar fraction of products in CH4 and CH4/H2 cycles.

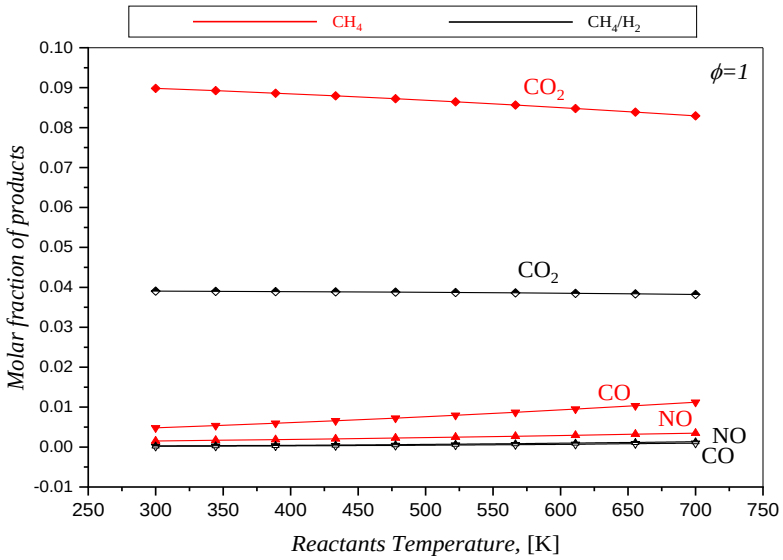

Fig.12. the impact of reactants temperature of CH4 and CH4/H2 cycles on molar fraction of combustion products in φ=1.

4.2.9. The impact of reactant NH_3 molar fraction on the thermodynamics parameters of Ammonia Brayton cycle

The impact of variation of reactant ammonia molar fraction on the some thermodynamic properties such as specific net work, thermal efficiency of ammonia cycle and equivalence ratio of ammonia Brayton cycle are examined, as shown in Fig. 13. According to the mentioned figure, increase of ammonia molar fraction from 0.10 to 0.2 leads in a dramatic growth of thermal efficiency from 52% up to 85%, while interval between molar fraction of 0.2 and 0.5 shows a decreasing path in which thermal efficiency falls down from 85% to 45%. As can be seen the ideal point for NH3 molar fraction is the point of 0.2, but there would occur a remarkable temperature rise, which needs more technical considerations.

On the other hand, increase of reactant NH3 molar fraction results in steady escalation of both the specific net work and equivalence ratio in ammonia Brayton cycle. As can be seen, at the lowest molar fraction of NH3, i.e. 0.1, the value of specific net work is just above 250 kJ/kg, which rises up to 3000 kJ/kg at the NH3 molar fraction of 0.5. In addition, a similar trend is shown for the equivalence ratio of ammonia Brayton cycle, by which the lowermost molar fraction of NH3, i.e. 0.1, stands in lean region of φ=0.7 and the uppermost molar fraction point of 0.5 is placed in rich region of φ=4.3. Furthermore, the optimum equivalence ratio of ammonia Brayton cycle, i.e. φ=1.2, is formed at the reactant NH3 molar fraction of 0.25.

4.2.10. The impact of variation of equivalence ratio on specific work output of proposed cycles

The impact of variation of equivalence ratio on specific work output of proposed cycles, including the steam Rankine, the ammonia Brayton and the methane-hydrogen Brayton cycles, are examined, as shown in Fig. 14. According to the figure, the equivalence ratio interval, $0.2 \leq \varphi \leq 1.5$, shows a general ascending trend over the all curves. Bothe the ammonia and methane/hydrogen Brayton cycles are place in almost similar quantity line in which at$\varphi = 0.2$, both the cycle hold the specific power under 100 kJ/kg. In addition, at the ending point, $\varphi = 1.5$, approximate value of specific for the both mentioned cycles stands just over 600 kJ/kg. However, the optimum $\varphi = 1$ for methane/hydrogen cycle shows specific work output of about 200 kJ/kg, ammonia Brayton cycle at optimum equivalence ratio, $\varphi = 1.2$, shows the stimated value of 400 kJ/kg.

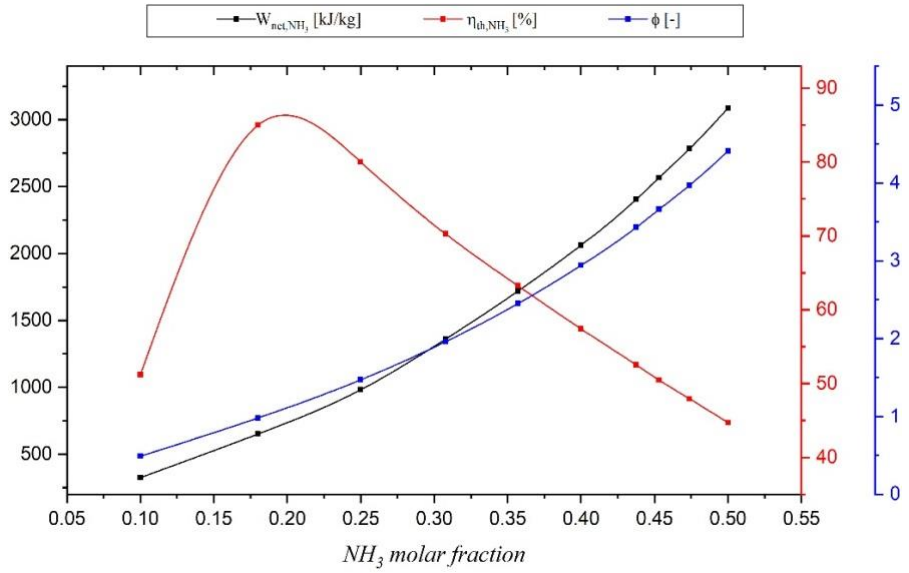

Fig.13. the impact of reactant NH3 molar fraction on the thermodynamics parameters of Ammonia Brayton cycle.

On the other hand, the subordinate steam Rankine cycle holds the utmost specific work, stem from the properties of water steam, and likewise the two mentioned cycles, it takes an ascending trend at $0.2 \leq \varphi \leq 1.5$. The least 2500 kJ/kg is gained at $\varphi = 0.2$ and the peak point of the route shows just under 5000 kJ/kg at $\varphi = 1.5$. Furthermore, the red curve is a summation of all three mentioned cycles, as total generated specific work in the proposed overall system. What is obvious is the direct relation of equivalence ratio with specific work in the mentioned cycles, which resulted from the growth of temperature inside the combustors and boiler as well.

4.2.11. The impact of variation of equivalence ratio on thermal efficiency of the proposed system.

The impact of variation of equivalence ratio on thermal efficiency of the proposed system was investigated, as illustrated in Fig. 15. In addition, the differences between the results of thermal efficiency in the present study with those of Keller et al. [43] was studied. According to the figure, the equivalence ratio interval, $0.2 \leq \varphi \leq 1.5$, displays a comparable movement over the two represented curvatures. Both the studies show ascending route in lean region and a falling trend inside the rich region. Accordingly, study of Keller et al., which is marked in blue curve, showed a chain of thermal efficiency between 48 and 63% for the combined cycle in their work. While at the point $\varphi = 0.2$ thermal efficiency of the system logged by 48%, the final equivalence ratio point, $\varphi \leq 1.5$, was palced in $\eta_{th,total} = 51\%$. The optimal limit of $\eta_{th,total}$ was located in the rich region, $1 \leq \varphi \leq 1.2$, which leaded in thermal efficiency of 57-63% .

On the other hand, the present study could improve the thermal efficiency of the overall proposed system, as shown in the figure. Accordingly, at the peak point, i.e. $\varphi = 1$, the overall thermal efficiency could improve by about 11% more than Kellers et al. study, to gain the value of $\eta_{th,total} = 74\%$. This is due to the linking the secondary Brayton cycle to the topping system, improvement in selection of reactant components molar fractions and some other thermodynamic parameters.

4.2.12. The impact of variation of equivalence ratio on NOx concentration at boiler outlet.

The impact of variation of equivalence ratio on NOx concentration at boiler outlet was analyzed, as shown in Fig. 16. Also, the dissimilarities amongst the consequences of NOx concentration in the current study with those of Keller et al. [43] was studied. According to the figure, the equivalence ratio interval, $0.2 \leq \varphi \leq 1.5$, shows a similar trend over the two shown curves. Ammonia

combustion provides various gaseous components such as OH, unburnt NH_3, NH_2, NH, N and NO. However, regarding to the results in this study the quantity of mentioned gases except NO were trivial and negligible. Hence, the relation of equivalence ratio with NO value was studied in this work.

According to the figure, the red curve illustrates the changes of NO in a study conducted by Keller et al. [43]. As can be seen, a rise and fall of NO concentration occurs by increasing of φ value. The starting point, $\varphi = 0.2$, logged the concentration of 35 ppm although this amount in present study is zero as shown in blue curve. The summit of NO value takes place through the lean region at $\varphi = 0.8$, in which Keller et al. logged the value of 2500 ppm, however at present study a fifty-percent decrease in nitrogen monoxide is shown down to the point of 1250 ppm.

While the rich region shows a falling trend, at the interval of $1.1 \leq \varphi \leq 1.5$, approximation to zero nitrogen monoxide can be seen. However, results of Keller et al. was placed in order of 30 to 50 ppm, our findings showed a declination of NO concentration down to 5 ppm at $\varphi = 1.1$. At the final point of equivalence ratio, NO values for Keller et al. and this work were 45 ppm and 18 ppm, respectively.

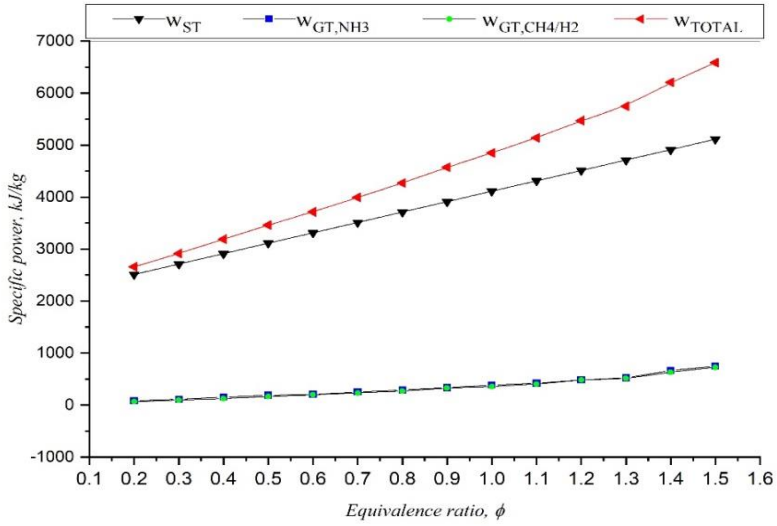

Fig.14. the impact of variation of equivalence ratio on specific work output of proposed cycles

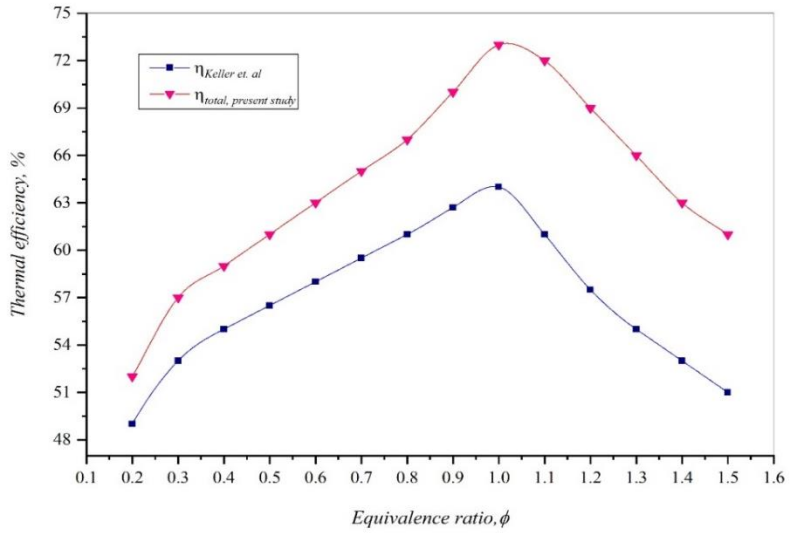

Fig.15. the impact of variation of equivalence ratio on thermal efficiency of the proposed system.

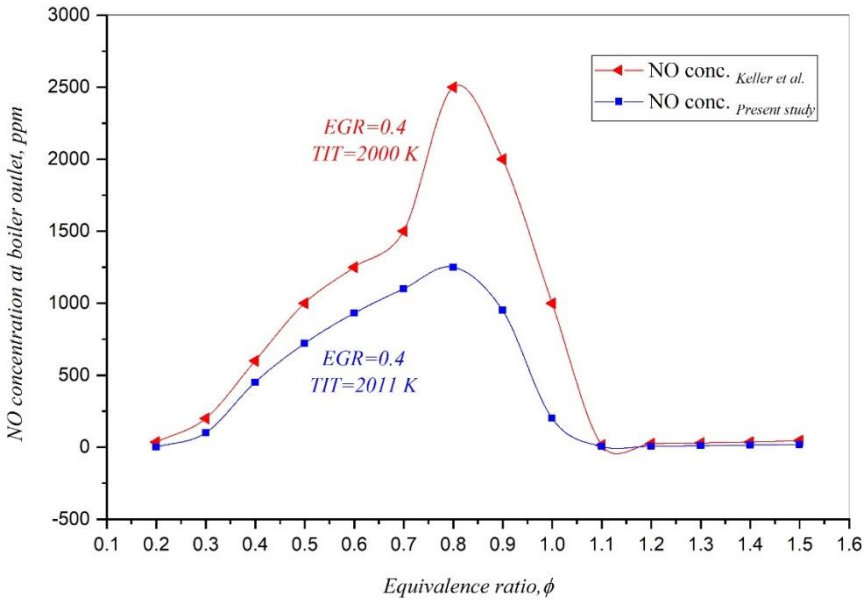

Fig.16. the impact of variation of equivalence ratio on NOx concentration at boiler outlet.

5. Conclusion

Nowadays, the increasing awareness on negative impacts of fossil fuels initiates the actions to towards the substitution of fossil fuels, by which the researchers comes to pursue and hire the carbon free fuels. Among the fuels with such unique features, ammonia and hydrogen are the notable ones by which the concept of clean energy power plants can be achievable.

In the current study, the chemical and thermodynamic analyses of the multi-fuel series of the integrated Brayton cycles as a combined heat and power plant was developed.

Hence, a novel system, consisting of the ammonia Brayton cycle with a subsidiary steam Rankine cycle and the methane/hydrogen-based Brayton cycle, is proposed. Using some chemical and thermodynamic software, GASEQ, ANSYS Chemkin and EES, the various compositions and properties of suggested fuel mixtures were analyzed. Then, the optimum molar fractions of the mixtures were selected considering the location of fuel in lean or rich regions. The literature showed some resolutions, but as the existing natural gas-based power plants are common across the world, the idea of NOx/Carbon free fuels encouraged us to improve the results of literature. Proposing an optimum scenario in which the least quantity of CO, CO2 and NOx species was discharged to the environment with a modification on thermal efficiency, was the main objective of this study.

In the parametric study, focused on a range of equivalence ratio (φ) as a key factor, different aspects of the proposed system were investigated, and after the analysis results, some concluding statements are multifold as follows:

- Ammonia combustion was a unique method to eliminate carbon emission, but the challenge of producing NOx particularly at higher thermal efficiency needs to select the innovative technologies and methods, of which the exact selection of reaction conditions can mitigate the NOx emission.
- Ammonia combustion causes a huge temperature inside the combustor, which challenges the feasibility of ammonia as a working fuel of power cycles. Then, this problem was solved with a low temperature exhaust gas recirculation (EGR). Once the cold EGR was added air without oxygen to cycles, the optimal combustion with lower temperature was achieved. The applicable range of EGR ratio varied between 0.4 and 0.6, in which the final combustion temperature

was 2011 K, at optimum equivalence ratio of 1.2.

- Hydrogen as a remarkable combustion products played a key role in mitigation of CO2 in methane/hydrogen cycle. 1-5 mol.% of hydrogen could notably decreased the release of CO and CO2 in methane/hydrogen Brayton cycle.
- At φ =1, using EGR=0.4 and mixture of methane/hydrogen resulted in decrease of CO2 down to 1 mol.%, while release of NO and CO dropped down to zero.
- Calculation proved a direct relation of NOx emission with thermal efficiency. Increase in thermal efficiency in ammonia cycle caused to growth of NOx production.
- Calculation verified an inverse relation of NOx emission with equivalence ratio in ammonia cycle. Increase in φ value in rich region caused to declination of NOx production.
- Increase of φ resulted in higher specific work of cycles. In ammonia cycle, at $\varphi = 1.2$ specific work cited by 1000 kJ/kg, and an improved thermal efficiency of 80%.
- Total thermal efficiency of proposed overall system in this study at $\varphi = 1$ was calculated by 74%, which is 11% more than 63% logged by Keller et al.
- The results showed that under the optimum operating conditions, at $\varphi = 1$, the thermal efficiency of methane/hydrogen Brayton cycle improved from about 36% up to 41.6%.
- The results showed no sizable improvement for the Steam Rankine cycle, as thermodynamic properties had not changed.
- The higher NO concentration at boiler outlet in lean region in this study was recorded by about 1200 ppm, while this number was 2500 ppm logged by Keller et al. In rich region, we experienced 10-ppm NOx value, while this was about 50 ppm in Keller et al. research. In addition, at $\varphi = 1$ this study could diminish the NO release from 1000 ppm to about 300 ppm.

As current study focused on chemical and energetic aspects of proposed system, considering other approaches such as exergy, exergoeconomic and exergoenvironmental analyses in future studies would present better insight over the proficiencies of the proposed system. In addition, regarding to the steam generation in boiler and HRSG connected to methane/hydrogen system, total site concept can be considered to tradeoff the existing utilities in current work.

References

[1] Valeria-Medina A.; S. Morris; J. Runyon; DG. Pugh; R. Marsh; P. Baesley; T. Hughes, "Ammonia, methane and hydrogen for gas turbines," Energy Procedia, vol. 75, pp. 118-123, 2015.

[2] Zamfirescu C, Dincer I., "Using ammonia as a sustainable fuel," Journal of Power Sources, vol. 185, pp. 459-465, 2008.

[3] Giddey S, Badwal SPS, Munnings C, Dolan M., "Ammonia as a renewable energy transportation media.," ACS Sustainable Chem Eng, pp. 10231-10239, 2017.

[4] Valera-Medin, A; Xiao, H; Owen-Jones, M; David, W.I.F.; Bowen , P.J., "Ammonia for power," Progress in Energy and Combustion Science, vol. 69, p. 63–102, 2018.

[5] Morgan E , Manwell J , McGowan J ., "Wind-powered ammonia fuel production for remote islands: a case study.," Renewable Energy, vol. 72, pp. 51-61, 2014.

[6] Zamfirescu, C.; Dincer, I., "Ammonia as a green fuel and hydrogen source for vehicular applications," Fuel Process Technol, vol. 90, p. 729–37, 2009.

[7] Zamfirescu C , Dincer I ., "Using ammonia as a sustainable fuel.," J Power SourceS, vol. 185, p. 459–465, 2008.

[8] Ravishankara AR , Daniel JS , Portmann RW ., "Nitrous oxide (N2O): the dominant ozone-depleting substance emitted in the 21st century," Science, vol. 326, p. 123–125, 2009.

[9] Nozari H, Karabeyoglu A., "Numerical study of combustion characteristics of ammonia as a renewable fuel and establishment of reduced reaction

mechanisms.," Fuel, vol. 159, pp. 223-233, 2015.

[10] Valera-Medina A, Pugh DG, Marsh P, Bulat G, Bowen P., "Preliminary study on lean premixed combustion of ammonia-hydrogen for swirling gas turbine combustors," Int J Hydrogen Energy, vol. 72, pp. 24495-503, 2017.

[11] Valera-Medina A, Gutesa M, Xiao H, Pugh D, Giles A, Goktepe B, et al., "Premixed ammonia/hydrogen swirl combustion under rich fuel conditions for gas turbines operation.," Int J Hydrogen Energy, vol. 44, pp. 8615-26., 2019.

[12] Karabeyoglu A, Evans B, Stevens J, Cantwell B., "Development of Ammonia Based Fuels for Environmentally Friendly Power Generation,," in 10th Ann Int Energy Conv Eng Conf, IECEC, 2012.

[13] Grcar JF, Glarborg P, Bell JB., Loren A, Jensen AD., "Effects of Mixing on Ammonia Oxidation in Combustion Environment Intermediate Temperatures," in Int Symp Combust., 2004.

[14] Ahlgren, W.,, "Fuel power density," Journal of Pressure Vessel Technology, vol. 134, no. 5, p. 054504, 2012.

[15] Bicer, Y., Dincer, I., Zamfirescu, C., Vezina, G., Raso, F., "Comparative life cycle assessment of various ammonia production methods," Journal of Clean Production, vol. 135, pp. 1379-1395, 2016.

[16] M. Guteša Božo; Mashruk, S.; Zitouni, S.; Valera-Medina, A., "Humidified ammonia/hydrogen RQL combustion in a trigeneration gas turbine cycle," Energy Conversion and Management, vol. 227, p. 113625, 2021.

[17] Guteša Božo, M.; Vigueras-Zuniga, MO.; Buffi, M.; Seljak, T.; Valera-Medina A., "Fuel rich ammonia-hydrogen injection for humidified gas turbines," Applied Energy , vol. 251, p. 113334, 2019.

[18] Valera-Medina, A.; Gutesa, M.; Xiao, H.; Pugh, D.; Giles, A.; Goktepe, B.; Marsh, R.; Bowen, P., "Premixed ammonia/hydrogen swirl combustion under rich fuel conditions for gas turbines operation," International Journal of Hydrogen Energy, vol. 44, no. 16, pp. 8615-8626, 2019.

[19] Aditya, K.M; Lim, W.O., "Investigation of ammonia homogenization and NOx reduction quantity by remodeling urea injector shapes in heavy-duty diesel engines," Applied Energy, vol. 323, p. 119586, 2022.

[20] Rahman, Z.; Wang, X.; Mikulcic H.; Zhou, S.; Zhang, J.; Vujanovic, M.; Tan, H., "Numerical assessment of NOx evolution in ammonia oxidation and its control by reburning in pressurized oxy-combustion," Journal of the Energy Institute, vol. 100, pp. 89-98, 2022.

[21] Mohammadpour A.; Mazaheri K.; Alipoor A., "Reaction zone characteristics, thermal performance and NOx/N2O emissions analyses of ammonia MILD combustion," International Journal of Hydrogen Energy, vol. 47, no. 48, pp. 21013-21031, 2022.

[22] Ni S.; Zhao D., "NOx emission reduction in ammonia-powered micro-combustors by partially inserting porous medium under fuel-rich condition," Chemical Engineering Journal, vol. 434, p. 134680, 2022.

[23] Ni, S.; Zhao D.; You, Y.; Huang, Y.; Wang, B.; Su, Y., "NOx emission and energy conversion efficiency studies on ammonia-powered micro-combustor with ring-shaped ribs in fuel-rich combustion," Journal of Cleaner Production , vol. 320, p. 128901, 2021.

[24] Han, L.; Li, J.;Zhao, D.; Xi, Y.; Gu, X.; Wang. N., "Effect analysis on energy conversion enhancement and NOx emission reduction of ammonia/hydrogen fuelled wavy micro-combustor for micro-thermophotovoltaic application," Fuel, vol. 289, p. 119755, 2021.

[25] Ariemma, G.B.; Sorrentino, G.; Ragucci, R.; Joannon, M.; Sabia, P., "Ammonia/Methane combustion: Stability and NOx emissions," Combustion and Flame, vol. 241, p. 112071, 2022.

[26] Matsumoto, H.; Kurahashi, K.; Tachikawa, H.; TakayaIseki, "Synthesis and Assessment of NOx to Ammonia Conversion Process in Combined Cycle Power Generation Systems," Computer Aided Chemical Engineering, vol. 49, pp. 253-258, 2022.

[27] Ma, P.; Huang,Q.; Si, T.; Yang, Y.; Li, S., "Experimental investigation of NOx emission and ash-related issues in ammonia/coal/biomass co-combustion in a 25-kW down-fired furnace," Proceedings of the Combustion Institute, 2022.

[28] Ni, S.; Zhao, D.; Wu, W.; Guan, Y., "NOx emission reduction reaction of ammonia-hydrogen with self-sustained pulsating oscillations," Thermal Science and Engineering Progress , vol. 19, p. 100615, 2020.

[29] Okafor, E.C.; Kunkuma, K.D.; Somarathne, A.; Ratthanan, R.S.; Hayakawa, A.; et al., "Control of NOx and other emissions in micro gas turbine combustors fuelled with mixtures of methane and ammonia," Combustion and Flame, vol. 211, pp. 406-416, 2020.

[30] "Ammonia injection failure diagnostic and correction in engine after-treatment system by NOx and NH3 emissions observation," Fuel, vol. 322, p. 123936, 2022.

[31] Wang, G.; Guiberti, T.F.; Cardona, S.; Avila C.; William, J.; Roberts, L., "Effects of residence time on the NOx emissions of premixed ammonia-methane-air swirling flames at elevated pressure," Proceedings of the Combustion Institute, 2022.

[32] Liu, W.; Long, Y.; Zhang, J.; Liu, S.; Zhou, Y.; et al., "Ag-Cu modified ZSM-5 zeolite to effectively eliminate NOx and slip ammonia from coal-fired flue gas: Catalytic performance and characterization," Journal of Environmental Chemical Engineering, vol. 10, no. 5, p. 108461, 2022.

[33] Xiao, R.;Zhang, J.F.; Zhao, L.K., "An ammonia-free denitration method: Direct reduction of NOx over activated carbon promoted by Cu-K bimetals," Journal of Fuel Chemistry and Technology, vol. 50, no. 5, pp. 628-639, 2022.

[34] Bykov, V.; Stein, M.; Maas, U., "Study of mechanism of ammonia decomposition and oxidation: From NOx reduction to ammonia auto-ignition problem," Proceedings of the Combustion Institute, 2022.

[35] Yaliwal, V.S.;Banapurmath, N.R.; Elahi, M.;Soudagar, M.;Afzal, A.; Ahmadi, P., "Effect of manifold and port injection of hydrogen and exhaust gas recirculation (EGR) in dairy scum biodiesel - low energy content gas-fueled CI engine operated on dual fuel mode," International Journal of Hydrogen Energy, vol. 47, no. 10, pp. 6873-6897, 2022.

[36] Wang, S.; Zhai, Y.; Wang, Z.; Hou, R.; Zhang,T.; Ji, C., "Comparison of air and EGR with different water fractions dilutions on the combustion of hydrogen-air mixtures," Fuel, vol. 324, no. Part B, p. 124686, 2022.

[37] Shen, W.; Xing, C.;Liu, H.; Liu, L.; Hu, Q.; Wu, G.; Yang, Y.; Wu, S.; Qiu, P., "Exhaust gas recirculation effects on flame heat release rate distribution and dynamic characteristics in a micro gas turbine," Energy, vol. 249, p. 123680, 2022.

[38] Lu, Z.; Liu, M.; Shi, L.; Wang. T.; Lu, T.; Wang, H., "Numerical research of the injected exhaust gas recirculation strategy on a two-stroke low-speed marine diesel engine," Energy, vol. 244, p. 122731, 2022.

[39] Rešetar, M.; Pejić, G.; Ilinčić, P.; Kozarac, D.; Lulić, Z., "Increase in nitrogen oxides due to exhaust gas recirculation valve manipulation," Transportation Research Part D: Transport and Environment, vol. 109, p. 103391, 2022.

[40] Hachem, J.; Schuhler,T.; Orhon,D.; Sjostrand, MC.; Zoughaib,A .; Molière, M., "Exhaust gas recirculation applied to single-shaft gas turbines: An energy and exergy approach," Energy , vol. 238, no. Part B, p. 121656, 2022.

[41] Ditaranto, M.; Heggset, T.; Berstad, D., "Concept of hydrogen fired gas turbine cycle with exhaust gas recirculation: Assessment of process performance," Energy , vol. 192, p. 116646, 2020.

[42] Rosec, Z.; Katrašnik, T.; Baškovič, UZ.; Seljak, T., "Exhaust gas recirculation with highly oxygenated fuels in gas turbines," Fuel , vol. 278, p. 118285, 2020.

[43] Keller M, Koshi M, Otomo J, Iwasaki H, Mitsumori T, Yamada K., "Thermodynamic evaluation of an ammonia-fueled combined-cycle," Energy , vol. 194, p. 116894, 2020.

[44] S. 6. National Institute of Standards and Technology. NIST Chemistry WebBook, "Thermophysical Properties of fluid

systems," NIST, 2018. [Online]. Available: https://webbook.nist.gov/chemistry/fluid/.

[45] G Tsatsaronis, T Morosuk, "Advanced thermodynamic (exergetic) analysis," J. Phys.: Conf. Ser. , vol. 395 , p. 012160, 2012.

[46] Pirmohamadi, A.; Ghaebi, H.; Ziapour, BM.; Ebadollahi, M., "Exergoeconomic Analysis of a Novel Hybrid System by Integrating the Kalina and Heat Pump Cycles with a Nitrogen Closed Brayton System," Energy Reports, vol. 7, p. 546–564, 2021.